REAL STRUCTURE AND RESIDUAL STRESSES IN ADVANCED WELDS DETERMINED BY X-RAY AND NEUTRON DIFFRACTION ANALYSIS

K. Trojan[1], J. Čapek[1], Ch. Hervoches[2], N. Ganev[1], P. Mikula[2], K. Kolařík[1]

[1]CTU in Prague, Department of Solid State Engineering, Faculty of Nuclear Sciences and Physical Engineering, Trojanova 13, 120 00 Prague 2, Czech Republic

[2]Nuclear Physics Institute, ASCR, v.v.i., Department of Neutron Physics, 25068 Řež, Czech Republic

Karel.Trojan@fjfi.cvut.cz

Keywords: X-ray diffraction, neutron diffraction, real structure, residual stresses, laser and MAG welding

Abstract

The aim of this paper is to describe the effects of laser welding on the real structure and residual stresses of construct steel S355 in comparison with classical arc welding. Therefore, results outline the capability of the advanced laser welding for joining thick sheets of steel using neutron diffraction and X-ray diffraction. This paper describes the effects of welding on the state of residual stresses and the real crystallographic structure (phase composition, crystallite size, microstrain) on cross-section of welds. Furthermore, the results of neutron diffraction verify previous assumptions of residual stresses redistribution as a result of the surface preparation for determination by X-ray diffraction in two directions on the cross-section of the welds.

Introduction

Laser processing is nowadays widely used in modern industry, mainly because of its high productivity and precision. Developed laser welding methods using high power lasers took over the capability to fill groove with cold or hot metal wire from arc welding. This leads to change in mechanical properties of welds, especially reducing their hardness due to quenching [1]. Profitable changes of real crystallographic structure (phase composition, crystallite size, microstrain) and residual stresses (RS) in comparison with conventional laser welds improve the results during impact and tensile test and mainly enhance fatigue life. This has been shown in the article [2].

Residual stresses are the stresses which occur in the material without the action of external forces. State of residual stress may be one of the most important factors that influence the behaviour of the material, especially fatigue life. Generally, it can be remarked, that mainly high compressive residual stresses could increase yield loads, promote crack initialization and also decelerate its propagation. So it is essential to achieve such a state of residual stress by applying various mechanical and thermal processing, which exhibits favourable residual stresses in critical areas of the component [3]. Residual stresses due to shrinking process are affected by the deformation of the component and the local shrinkage processes according to the thermal expansion coefficient of the using material. On the other hand, when considering a phase transformation from austenite to ferrite, bainite, or martensite, it is associated with a characteristic volume increase. This effect is caused by the change of the close-packed face-centered cubic (fcc) crystal structure to the body-centered cubic (bcc) crystal structure or body-centered tetragonal (bct), respectively. This expansion takes place during the phase transformation proceeds in the restrained volume thus compressive residual stresses are formed [4].

Experimental

The analysed butt-welds were prepared by a double sided laser welding with cold wire and multilayer double side metal active gas (MAG) welding from two 300×150×20 mm^3 sheets made of S355J2 steel. The measurements were performed on the cross-section of the welds in three lines perpendicular to the welds. One line passes through the centre of the weld and the other two are located three millimetres below each surface. The side with the upper line was welded first. To determine the real structure and RS by X-ray diffraction (XRD) on the cross-section, it was necessary to cut the plate in two parts and the affected surface layer electrochemically etched. RS determined by neutron diffraction were obtained non-destructively without cutting. Sample orientations during X-ray and neutron diffraction are shown in Fig. 1. The direction of the arrows always indicates the direction of the measured RS.

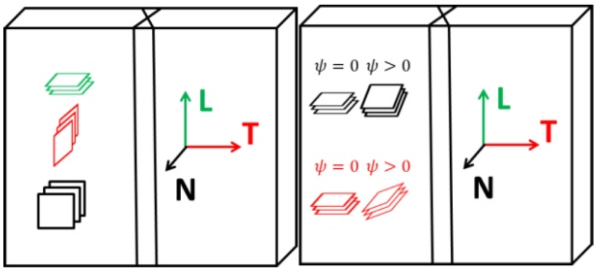

Figure 1. Sample orientations and analysed planes during neutron diffraction (left) and XRD (right).

The neutron measurements were carried out on the diffractometer SPN-100 of the Nuclear Physics Institute which is installed at the channel HC-4 of the research reactor LVR-15 and operates at the neutron wavelength of 0.235 nm. The diffraction peak {110} of -Fe was measured. The SteCa software [5] was used to extract and analyse diffraction patterns from the recorded area detector data. The stress was calculated using the Hooke's law based on the angular deviation of the diffraction profile position from the value related to the stress-free sample. The irradiated volume was approximately 2 × 2 × 3 mm^3.

The corresponding XRD measurements were performed by *PROTO iXRD COMBO* diffractometer with -goniometer and {211} diffraction line of -Fe was measured by chromium radiation. Deformation of interplanar distances of variously rotated planes (according to the angle , see Fig. 1 right) was converted to RS using the generalized Hooke's law according to the method. Diffraction

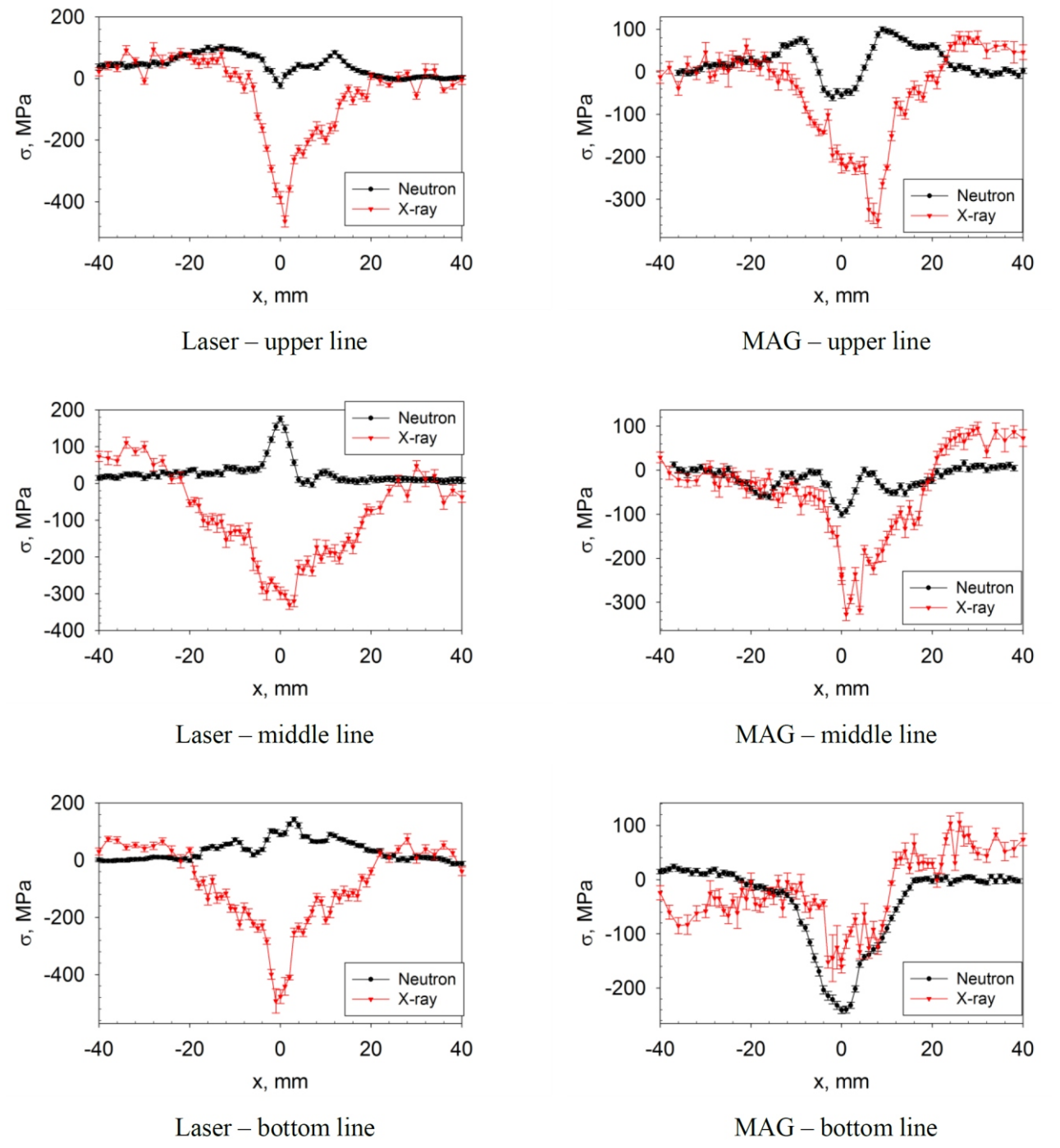

Figure 2. Comparison of RS obtained by X-ray and neutron diffraction in direction perpendicular to the weld for laser (left column) a MAG sample (right column).

angle 2 ^{211} was taken as a centre of gravity of the {211} diffraction doublet CrK . For residual stress evaluation, X-ray elastic constants $\frac{1}{2}s_2 = 5.76$ TPa^{-1} and $s_1 = -1.25$ TPa^{-1} were used. The effective depth of penetration (T^{eff}) is corresponding to the thickness of a surface layer that provides about 63 % of the diffracted intensity. In the case the T^{eff} is about from 3.5 up to 5.5 m.

In order to determine the phase composition, diffraction patterns were obtained by measuring the welds using the *X'Pert PRO MPD* instrument in classical Bragg-Brentano focusing configuration with cobalt tube anode and mono-capillary with a diameter 0.5 mm. Measured diffraction diagrams were processed with the program *X'Pert HighScorePlus* and crystalline phases were identified using a *PDF-2* database. Quantitative analysis was evaluated using the Rietveld analysis in the *TOPAS 4.2* software. In the case of the used wavelength, the T^{eff} is about 5 m.

Results and discussion

The comparison of RS obtained by neutron and X-ray diffraction in normal and perpendicular direction to the weld is plotted for both samples in Figs. 2 and 3. Phase compositions were determined on the cross sections, where the weight representation of retained austenite (see Fig. 4), microstrain (see Fig. 5) and crystallite size (see Fig. 6) were

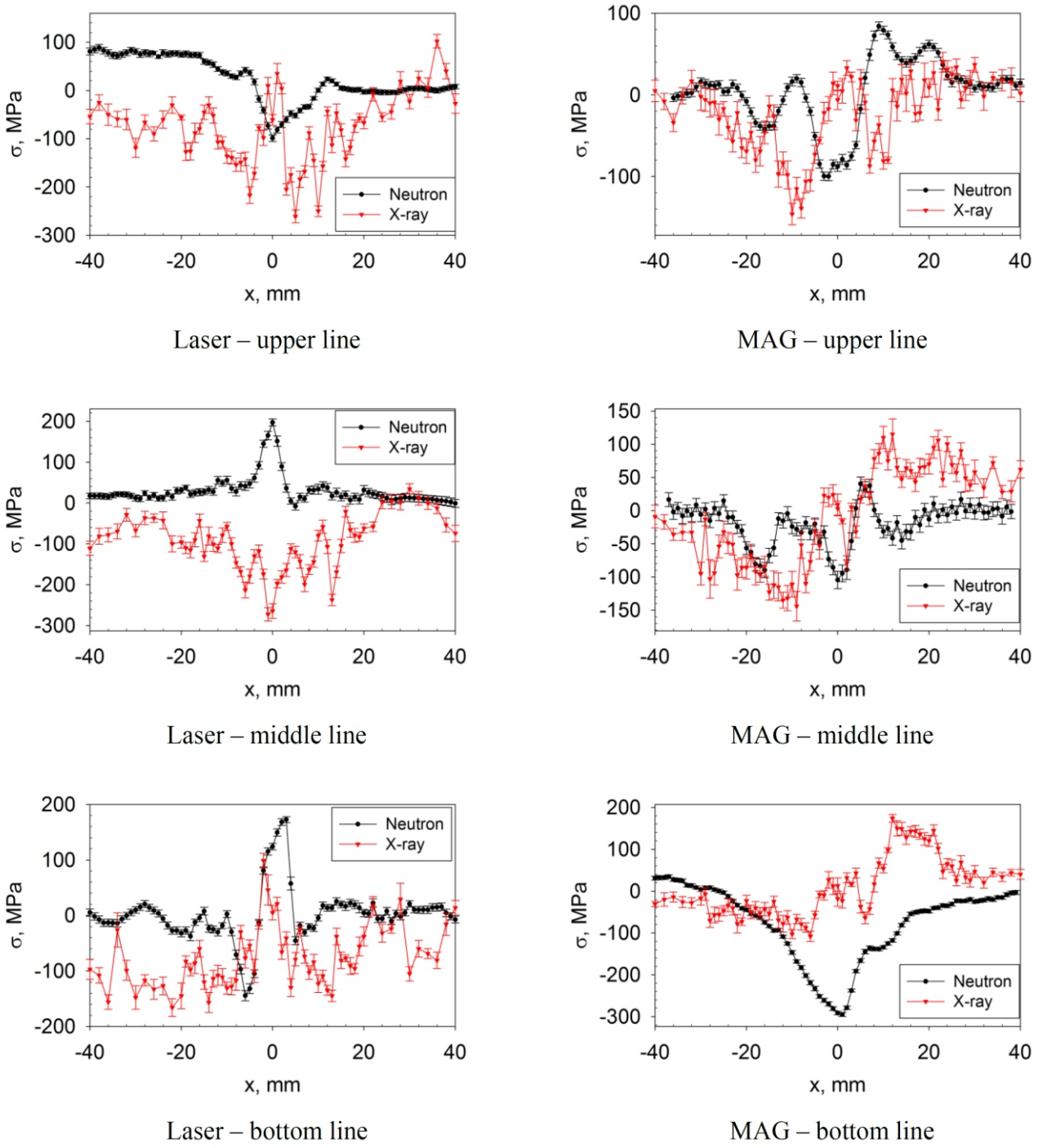

Figure 3. Comparison of RS obtained by X-ray and neutron diffraction in normal direction to the weld for laser (left column) a MAG sample (right column).

evaluated by Rietveld analysis. In the graphs, the centre of the welds is given by zero on the x-axis.

In the middle of the laser weld in direction T according to Fig. 2, RS obtained by neutron diffraction in the perpendicular direction to the weld reported more tension character than obtained by XRD. This is most probably due to a significant contraction in the direction parallel to the weld. On the other hand in the case of the MAG weld, there are compressive RS. This could suggest a predominance of phase transformation during the formation of RS rather than shrinkage. For both welds, RS obtained by XRD reported higher compressive results than obtained by neutron diffraction. The only exception is the bottom line for the MAG weld. The asymmetric course of RS for MAG sample is mainly due to the fact that the grove was filled with another bead in the right part from the both sides (position of this beads were approx. 5 mm from the centre).

Laser weld (according to the previous results [6]) has a higher tensile residual stresses along the weld, therefore, redistribution after cutting the sample probably produced the greatest compressive stresses analysed by XRD. After cutting the plate in two parts, the weld probably slightly dropped, and thus it caused compressive RS in the plane perpendicular to the weld.

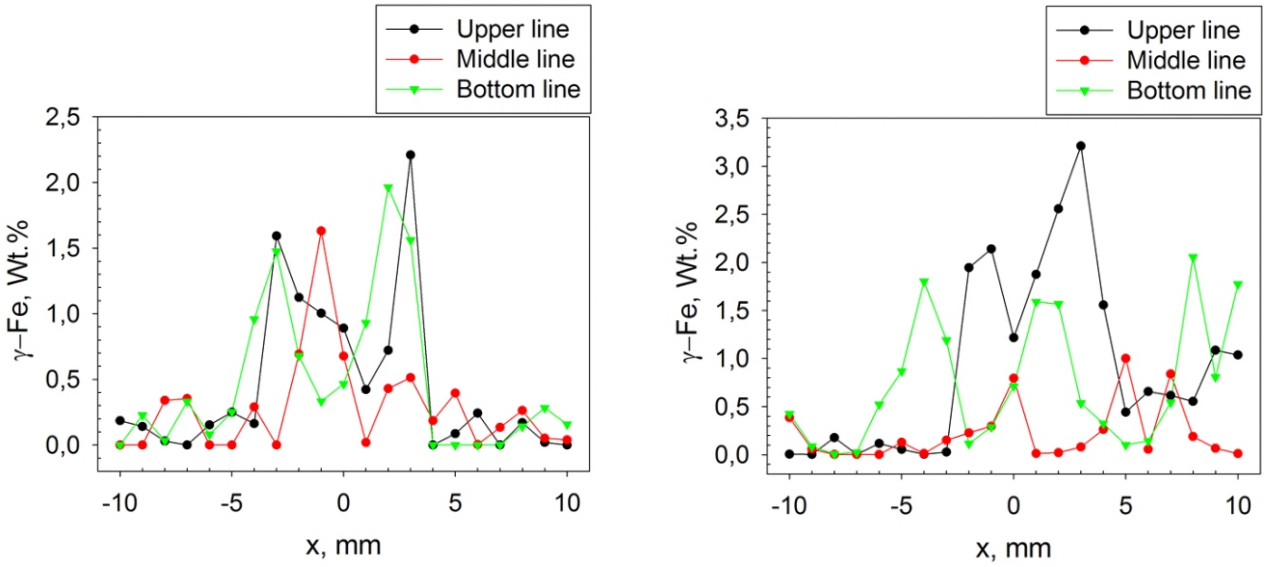

Figure 4. Comparison of weight percentage of retained austenite for laser (left) a MAG sample (right).

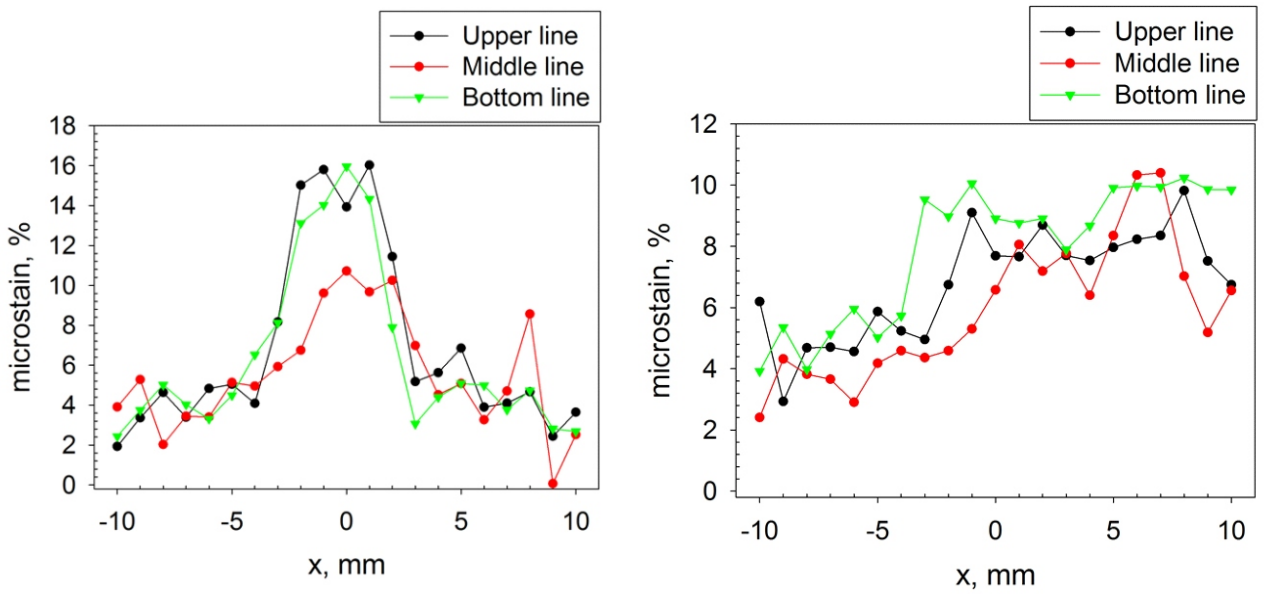

Figure 5. Comparison of microstrain for laser (left) a MAG sample (right).

In the middle of the laser weld in normal direction according to Figs. 3, RS obtained by neutron diffraction reported as well tension character. MAG sample in the middle line exhibits much better correspondence. The greatest difference observed for MAG weld is at the bottom line, where XRD showed slight tensile residual stresses and neutron diffraction compressive ones. The same asymmetric course of RS for MAG sample is also clearly visible for normal direction in Fig. 3.

The dependency of retained austenite (see Fig. 4) for the laser weld copies the boundary between the melt pool and the heat affected zone (HAZ) where the cooling was the fastest. However, for middle line of the MAG sample, where a first layer was welded, almost no retained austenite was detected. This is most likely caused by heating by other welding beads, when a larger amount of heat input was added to the weld in comparison with laser welding. Higher values of retained austenite for the upper and bottom lines on the right side are given by the same reason as for RS, the groove was filled with another weld bead in this area. For the laser sample, the weld width is approximately 4 mm on both sides. Unfortunately, the width for the MAG sample is from –5 mm to more than 10 mm.

From a crystallite size (see Fig. 6), it is possible to notice that slightly higher values could be seen in the HAZ with the laser middle line exception. In the HAZ, due to heat input, the crystallites are coarsening. This effect is better observable for MAG weld as there was higher heat input. On the other hand, the microstrain for the laser weld (see Fig. 5) reaches the highest values in the middle of the original melt pool. For MAG weld, microstrains also grow, but values are lower than for the laser sample. Higher microstrain values are most likely due to a higher cooling rate and thus a non-equilibrium microstructure is formed.

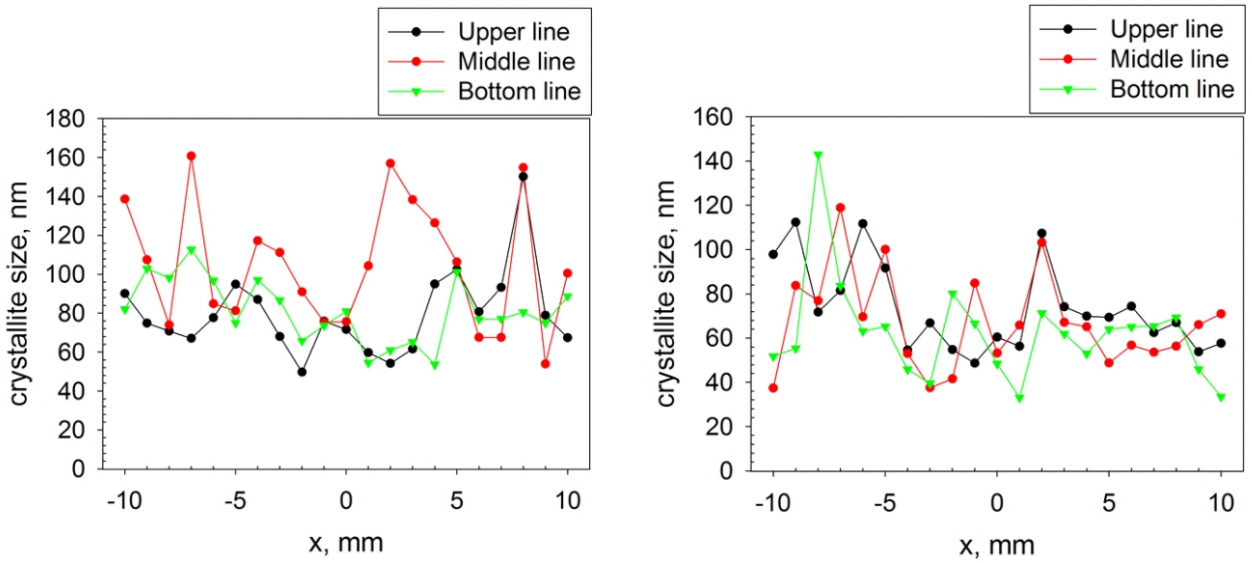

Figure 6. Comparison of crystallite size for laser (left) a MAG sample (right).

Conclusion

The resulting RS obtained using both methods with a different approach are in clear correlation. The redistribution of RS during the cutting has not yet been accurately described. But it can be deduced from these presented results that the preparation of the cross-section for XRD measurements of the welds did not significantly change the distribution of residual stresses in the cutting plane. They had been only partially affected. However, the redistribution of residual stress after cutting must be taken into acount. The microstrain for the laser weld exhibits the highest values than for MAG weld. In contrast, the slightly higher values were determined in the HAZ for both samples.

From our point of view, X-ray diffraction is a suitable instrument to describe the real structure and state of residual stress even for the cross-section of such thick steel plates. However, it is necessary to keep in mind that even the residual stresses in the plane of the cut are partially affected by the cross-section preparation. It is often assumed that the residual stresses in this plane are not affected, but it is not always the correct assumption even according to these results.

References

1. M. Sokolov, A. Salminen, M. Kuznetsov, I. Tsibulskiy, *Materials & Design*, **32**, (2011), pp. 5127-5131.
2. I. Černý, J. Sís, *Key Engineering Materials,* **713**, (2016), pp 82-85.
3. G. E. Totten, M. Howes, T. Inoue, *Handbook of residual stress and deformation of steel*. Materials Park: ASM International. 2002.
4. T. Nitschke-Pagel, K. Digler, *Materials science forum*, **783**, (2014), pp. 2777-2785.
5. C. Randau, U. Garbe, H.-G. Brokmeier, *Journal of Applied Crystallography*, 44, (2011), pp. 641–646.
6. K. Trojan, Ch. Hervoches, K. Kolařík, N. Ganev, P. Mikula, J. Čapek, *The 5th Student Scientific Conference on Solid State Physics, Sedliště 2016*, (2016), pp. 40-45.

Measurements were carried out at the CANAM infrastructure of the NPI ASCR Řež supported through MŠMT project No. LM2011019 and Czech Science Foundation GAČR through the project No. 14-36566G entitled as Multidisciplinary Research Centre for Advanced Materials. The authors thank to Doc. Němeček for supplying the laser weld. This work was supported by the Student Grant Competition CTU in Prague grant No. SGS16/245/OHK4/3T/14.